Available online at www.sciencedirect.com

SciVerse ScienceDirect

Ceramics International 39 (2013) S365–S368

CERAMICS INTERNATIONAL

www.elsevier.com/locate/ceramint

Preparation and electrical properties of $NaNbO_3$ ceramics synthesized by topochemical microcrystal conversion

Ali Hussain[a], Jin-Soo Kim[a], Gyung-Hyun Ryu[a], Tae-Kwon Song[a], Myong-Ho Kim[a,*], Won-Jeong Kim[b]

[a]School of Nano & Advanced Materials Engineering, Changwon National University, Gyeongnam 641–773, Republic of Korea
[b]Department of Physics, Changwon National University, Gyeongnam 641–773, Republic of Korea

Available online 23 October 2012

Abstract

$NaNbO_3$ (NN) ceramics were successfully synthesized from bismuth layer-structured $Bi_{2.5}Na_{3.5}Nb_5O_{18}$ (BNN) particles by a topochemical microcrystal conversion method. Plate-like BNN particles were first synthesized by molten salt synthesis (MSS) technique. After topochemical reaction with complementary reactant sodium carbonate (Na_2CO_3) in sodium chloride (NaCl) flux, the layer structure of BNN particles were transformed to NN perovskite structure. The crystal structure and microstructure of the synthesized particles were examined through XRD and SEM analysis, respectively. Dielectric, complex impedance and conduction behaviors of the sintered NN ceramics were investigated in the frequency range of 100 Hz–1 MHz at different temperatures (50–550 °C).

Keywords: A. Grain growth; B. Platelets; C. Electrical properties; D. Perovskites

1. Introduction

$(K, Na)_{0.5}NbO_3$ (KNN) based ceramics have become the focus of much research interest since Saito et al. [1] obtained high piezoelectric properties ($d_{33}=416$ pC/N and $k_p=0.61$) by reactive template grain growth (RTGG) method. However, KNN-based ceramics prepared by conventional solid state reaction (SSR) show poor piezoelectric properties ($d_{33}=80$ pC/N, and $k_p=0.36$) due to difficulty in obtaining high density ceramics [2,3].

$NaNbO_3$ (NN) is considered one of the most promising materials for texturing KNN-based ceramics. However, NN particles prepared by conventional mixed-oxide (CMO) method have equiaxial morphology which cannot satisfy the requirement as template in the RTGG process. Molten salt synthesis (MSS) is a well established technique to prepare particles with anisotropic morphology [4,5]. Another useful approach to prepare perovskite templates is topochemical microcrystal conversion (TMC) synthesis, which involves replacing or modifying the interlayer cations but retaining the morphological and structural features of plate-like layered-perovskite precursors by ion exchange and intercalation reactions at low temperatures [6,7].

In view of the importance of the NN templates for high performance lead-free textured KNN-based ceramics the present study is carried out to prepare and study the structure and electrical properties to better understand the underlying conduction mechanism.

2. Experimental procedure

Plate-like $Bi_{2.5}Na_{3.5}Nb_5O_{18}$ (BNN) precursors were prepared by MSS. Reagent-grade Bi_2O_3, Nb_2O_5 and Na_2CO_3 powders of purity (99.9%) were first mixed according to the formula of $Bi_{2.5}Na_{3.5}Nb_5O_{18}$ (BNN) for 12 h. The mixture was then mixed thoroughly with NaCl (99.95%) in the weight ratio of oxide to salt 1:1.5 for 12 h. After drying, the mixture was placed in a sealed alumina crucible, heated to 1125 °C for 4 h. After the completion of reaction, the as-synthesized product was washed several times with hot de-ionized water to remove NaCl salt. BNN platelets and Na_2CO_3 were weighed in molar ratio of

*Corresponding author. Tel.: +82 55 213 3711; fax: +82 55 262 6486.
E-mail address: mhkim@changwon.ac.kr (M-H. Kim).

0272-8842/$ - see front matter © 2012 Elsevier Ltd and Techna Group S.r.l. All rights reserved.
http://dx.doi.org/10.1016/j.ceramint.2012.10.095

BNN/Na_2CO_3 1:1.5, NaCl salt was added to them with 1:1.5 weight ratios, and then mixed with a magnetic stir bar for 6 h. The mixture was placed in a sealed alumina crucible, and heated at 950 °C for 4 h. The product was washed several times with hot de-ionized water. The NN template was separated using HCl to remove the by-product, Bi_2O_3. Finally, the obtained plate-like NN ceramics were pressed into pellets and sintered at 1250 °C for 4 h.

Crystallographic phases and surface morphology of the prepared samples were confirmed by XRD and SEM, respectively. For the measurements of the electrical properties, a 0.5 mm thick disk-shaped sample was covered with a thin layer of silver-palladium paste as electrodes and was fired at 700 °C for 30 min. The dielectric and the complex impedance data of the NN template ceramics were measured by an impedance analyzer (HP4192A) in the frequency range of 0.1 kHz to 1 MHz over a temperature range of 50–550 °C.

3. Results and discussion

Fig. 1(a), (b) shows the SEM micrographs of BNN and NN particles, respectively. The particles show an anisotropic platelet microstructure with pseudocubic or pseudotetragonal surface with high aspect ratio and high degree of orientation. The BNN particles prepared by the MSS method were used as precursor for NN templates through TMC method. It can be observed from Fig. 1(b) that the converted product preserve the morphology of BNN precursor and develop a (00l)-oriented tetragonal perovskite. These NN particles are believed to possibly be easily orientated in a matrix of fine powders by a shearing process (e.g. tape casting), resulting in well textured microstructure found in products obtained by TGG or RTGG processing.

The XRD pattern of NN particles transformed from the BNN precursor are shown in Fig. 2(a). It has a single phase perovskite structure with tetragonal symmetry. The perovskite type materials with intensity peak (200) at 2θ angle of 46.5° is characterized as a cubic phase, however the splitting of (200) into (002) and (200) at 2θ angle of 46.5° is the characteristic of tetragonal phase, which is identified by JCPDS nos. 75–2102 and 74–2455, respectively. The difference between the cubic phase and tetragonal phase is that in cubic phase Na^+ locates in the center of eight NbO_6 octahedra, while in tetragonal phase Na^+ deviate from the center of eight NbO_6 octahedra. At the higher soaking temperature, Na^+ of cubic NN deviates the center of eight NbO_6 octahedra because of

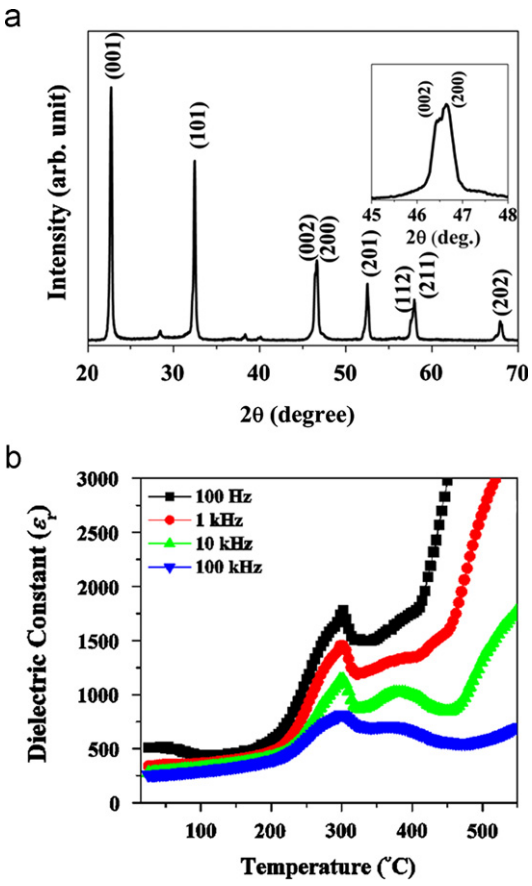

Fig. 2. (a) XRD patterns of plate-like NN particles synthesized from BNN precursor. (b) Temperature dependence of dielectric constant of NN ceramic at different frequencies.

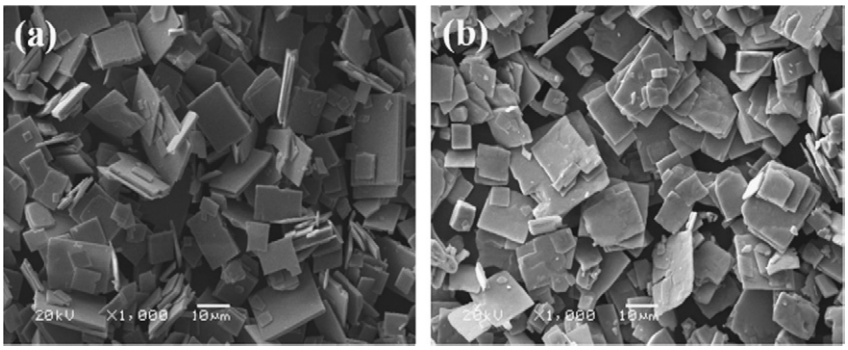

Fig. 1. SEM micrographs (a) BNN precursors synthesized by MSS. (b) NN templates synthesized by TMC.

distortion of crystal lattice, therefore, cubic phase of NN transforms into tetragonal phase of $NaNbO_3$.

The temperature dependence of dielectric constant of the NN ceramic at different frequencies (100 Hz – 100 kHz) is shown in Fig. 2(b). NN ceramics exhibit no obvious change at maximum permittivity temperature (T_m) with increase in measurement frequency showing a non relaxor behavior. However, T_m is observed at 300 °C, which is less than previously reported NN ceramics (350 °C) prepared by conventional methods [8], which may be due to different processing techniques.

Fig. 3(a) and its insets show the variation of real part (Z') of the complex impedance ($Z^*=Z'-jZ''$) with frequency at different temperatures. At lower temperature, Z' decreases with increasing frequency up to a certain frequency and then becomes frequency independent. Frequency dependence of imaginary part (Z'') of impedance at different temperatures is shown in Fig. 3(b). The Z'' is characterized by the appearance of peaks at high temperatures 400 °C and above. In addition, the broadening of the peak shifted towards higher frequencies as the temperature increased. A significant broadening of the peak with increasing temperature suggests a temperature dependent electrical relaxation phenomenon in the material [9]. The relaxation time ($\tau_{Z''}$) is the frequency at which the dielectric peak occurs in the impedance loss spectra. It was calculated from Fig. 3(b) using the equation: $\tau_{Z''}=1/2\pi f$ where f is the frequency of relaxation and presented in Fig. 3(c). Plot of $\tau_{Z''}$ vs. 1000/T follow Arrhenius law: $\tau_{Z''}=\tau_0 \exp(E_a/k_BT)$ where τ_o is the prefactor, E_a denotes the activation energy for the response and k_B is Boltzmann constant. From the slope of the linear fit, we obtain activation energy of 1.16 eV, a signature of oxygen vacancies, thus confirming their role in the mechanisms of conduction.

Fig. 4(a) and its inset show the plot of Z' versus Z'' (Cole–Cole or Nyquist plots) at different temperatures. With increase in temperature the slope of the line decreases and their curves move toward real (Z') axis. At higher temperatures i.e., above 350 °C, semicircles can be formed. The center of these semicircles lies below the x-axis, which means a non Debye relaxation. The complex impedance

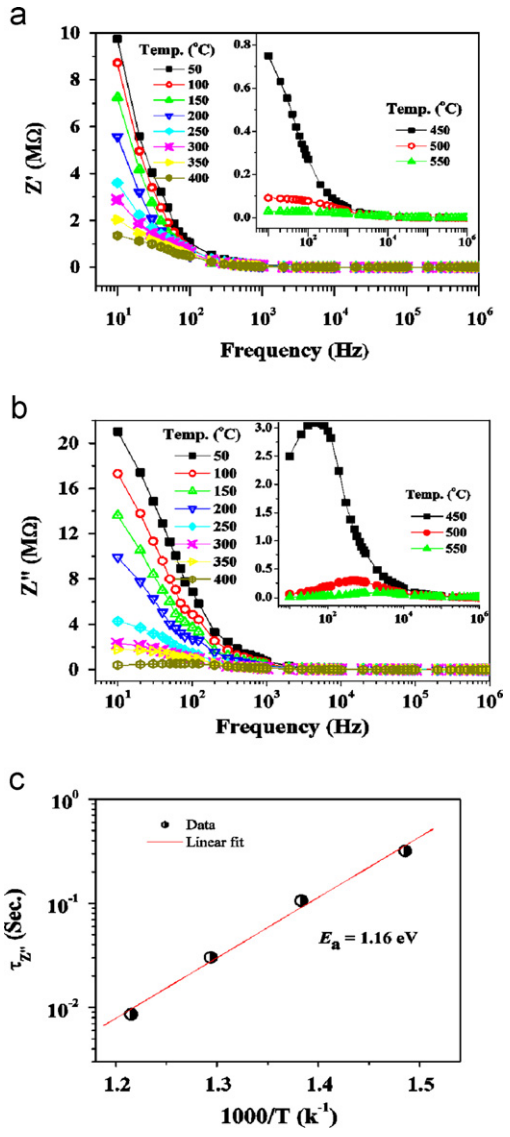

Fig. 3. (a) Variation of impedance real part (b) imaginary parts and (c) Arrhenius plot of the relaxation time $\tau_{Z''}$ from impedance spectra.

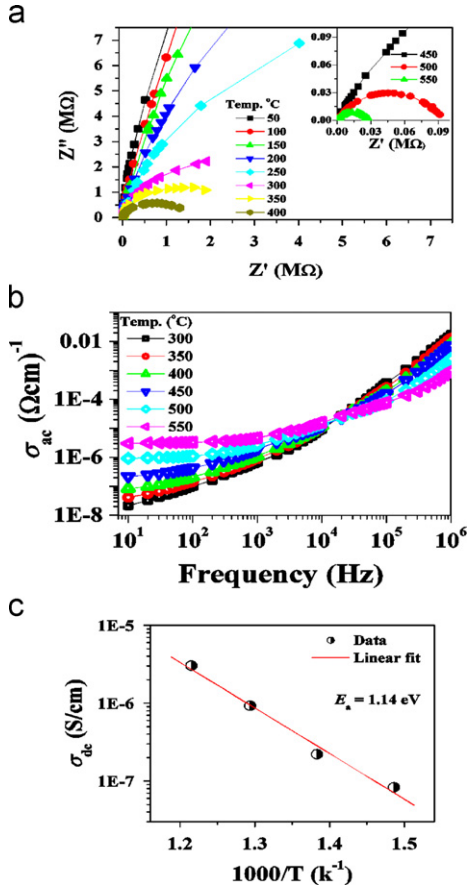

Fig. 4. (a) Cole–Cole (Nyquist) plots (b) ac conductivity of NN ceramic at different temperatures and (d) dc conductivity (σ_{dc}) as a function of 1000/T.

(Z^*) can be expressed by Cole–Cole equation: $Z^* = R/(1+(j\omega\tau_{Z''})^{\alpha})$, where $\tau_{Z''} = RC$ is the relaxation time, R and C are the resistances and capacitance, respectively, in a parallel circuit and α $(0 < \alpha \leq 1)$ quantifies the shift of response compared to a signature of Debye and characterize the distribution of the relaxation time [9,10]. In the impedance plot, a single semicircular arc with a single relaxation process was observed at temperatures of 400 °C and above, which confirms that the impedance contribution is mainly due to the grains. The effect of temperature on the impedance behavior of the sample becomes clearly visible from the pattern of the Nyquist plot. As the temperature increases, the intercept of the prominent semicircles at the Z′ axis shift toward lower Z′ value, indicating a reduction of grain impedance. At high temperatures 500 °C and above an indication of deviation from the semicircle is observed. This deviation may be related to the contribution of the grain boundaries due to its high resistance and high capacitance [11].

Fig. 4(b) shows the variation of ac conductivity as a function of frequency at different temperatures. At low frequency, the ac conductivity shows the existence of a plateau (σ_{dc}) independent on the frequency. At higher frequency, the ac conductivity increases with increasing frequency and obeying to a power law ($\sigma_{ac} \alpha \omega^n$) where n is the frequency exponent. This behavior is described by the well-known Jonscher power law [10]: $\sigma_{ac} = \sigma_{dc} + A\omega^n$, where A is a pre-exponential factor. The dc (bulk) conductivity (σ_{dc}) of the sample was evaluated from Fig. 4(b) and is shown in Fig. 4(c). The nature of the variation of σ_{dc} is linear and follows the Arrhenius relationship: $\sigma_{dc} = \sigma_o \exp(-E_a/k_B T)$, where E_a is the activation energy of conduction, k_B is Boltzmann's constant and T is the absolute temperature. The value of the activation energy (E_a) was calculated from the slope of the $\ln\sigma_{dc}$ versus 1000/T curve and found to be 1.14 eV. This value of E_a is approximately the same as the energy ($\sim$1 eV) required for the motion of oxygen vacancies. This confirms that the observed conductivity is due to the movement of oxygen vacancies in this material [12].

4. Conclusion

$NaNbO_3$ ceramics have been successfully synthesized from bismuth layered ferroelectric $Bi_{2.5}Na_{3.5}Nb_5O_{18}$ by a topochemical microcrystal conversion method. The XRD pattern of NN ceramics reveals the formation of pure perovskite phase. The surface morphology of the NN particles preserves the platelet morphology of the BNN precursor. At high temperature a single semicircular arc was observed in the impedance plot suggesting that the impedance relaxation is mainly due to grain. The relaxation time obeys Arrhenius equation having activation energy of 1.16 eV. The activation energy calculated from both dc conductivity curves was 1.14 eV, confirming that the conduction behavior is mainly due to the movement of oxygen vacancies.

Acknowledgments

This work was supported by Basic Science Research Program through the National Research Foundation of Korea (NRF) funded by Ministry of Education, Science and Technology (MEST) (2011–0030805).

References

[1] Y. Saito, H. Takao, T. Tani, T. Nonoyama, K. Takatori, T. Homma, T. Nagaya, M. Nakamura, Lead-free piezoceramics, Nature 432 (2004) 84–87.
[2] M.D. Maeder, D. Damjanovic, N. Setter, Lead-free piezoelectric materials, Journal of Electroceramics 13 (2004) 385–392.
[3] L. Egerton, D.M. Dillon, Piezoelectric and dielectric properties of ceramics in the system potassium-sodium niobate, Journal of the American Ceramic Society 42 (1959) 438–442.
[4] Z. Li, X. Zhang, J. Hou, K. Zhou, Molten salt synthesis of anisometric $Sr_3Ti_2O_7$ particles, Journal of Crystal Growth 305 (2007) 265–270.
[5] Y. Kan, X. Jin, P. Wang, Y. Li, Y. Cheng, D. Yan, Anisotropic grain growth of $Bi_4Ti_3O_{12}$ in molten salt fluxes, Materials Research Bulletin 38 (2003) 567–576.
[6] E.S. Raymond, E.M. Thomas, Topochemical synthesis of three dimensional perovskites from lamellar precursors, Journal of the American Chemical Society 122 (2000) 2798–2803.
[7] S. Borg, G. Svensson, J. Bovinw, Structure Study of $Bi_{2.5}Na_{0.5}Ta_2O_9$ and $Bi_{2.5}Na_{m-1.5}Nb_mO_{3\ m+3}$ (m=2–4) by neutron powder diffraction and electron microscopy, Journal of Solid State Chemistry 167 (2002) 86–96.
[8] S. Lanfredi, M.H. Lente, J.A. Eiras, Phase transition at low temperature in $NaNbO_3$ ceramic, Applied Physics Letters 80 (2002) 2331–2333.
[9] S.K. Barik, P.K. Mahapatra, R.N.P. Choudhary, Structural and electrical properties of $Na_{1/2}La_{1/2}TiO_3$ ceramics, Applied Physics A 85 (2006) 199–203.
[10] A.K. Jonscher, Dielectric relaxation in solids, Journal of Physics D: Applied Physics 32 (1999) 57–70.
[11] J. Liu, C.G. Duan, W.G. Yin, W.N. Mei, R.W. Smith, J.R. Hardy, Large dielectric constant and Mawell–Wagner relaxation in $Bi_{2/3}Cu_3Ti_4O_{12}$, Physical Review B 70 (2004) 144106–144107.
[12] S. Sen, R.N.P. Choudhary, P. Pramanik, Structural and electrical properties of Ca^{2+}-modified PZT electroceramics, Physica B-Condensed Matter 387 (2007) 56–62.